Int J Clin Exp Med 2017;10(8):11912-11920
www.ijcem.com /ISSN:1940-5901/IJCEM0055216

Original Article

Localization of nerve entry point and intramuscular nerve-dense regions as targets to block brachioradialis muscle spasticity

Shengbo Yang[1], Shuaiyu Hu[1], Bangguo Li[2], Xiaomei Li[3]

[1]Department of Anatomy, Zunyi Medical College, Zunyi, People's Republic of China; Departments of [2]Radiology, [3]Rehabilitation Medicine, The First Affiliated Hospital of Zunyi Medical College, Zunyi, Guizhou, People's Republic of China

Received April 12, 2017; Accepted June 7, 2017; Epub August 15, 2017; Published August 30, 2017

Abstract: This study aimed to identify the location and depth of the nerve entry point (N_1) and center of the intramuscular nerve-dense region (N_2) of the brachioradialis muscle. Using 40 upper limbs from 20 adult cadavers, curved lines joining (1) the lateral epicondyle of the humerus and acromion and (2) the lateral epicondyle of the humerus and styloid process of the radius were designated as longitudinal reference lines (L_1 and L_2) of N_1 and N_2, respectively. The curved line joining the lateral and medial epicondyle of the humerus was the common horizontal reference line (H). N_2 was stained with Sihler's stain. N_1 and N_2 were labeled with barium sulfate, and their body surface projection points (P_1 and P_2) were determined by spiral computed tomography. Projection of N in the opposite direction was designated P'. The percentage location of the intersections (P_H and P_L) of P with L and H lines, and the percentage depth of N were determined. P_{1L} and P_{1H} were at 9.33% of L_1 and 30.69% of H, respectively. N_1 was at 31.03% of P_1P_1'. There were two N_2 regions in the brachioradialis muscle. P_{2L} of the proximal N_2 (PN_2) and distal N_2 (DN_2) was located at 12.60% and 40.74% of L_2, and P_{2H} at 25.12% and 32.86% of H, respectively. PN_2 and DN_2 were at 5.99% and 8.99% of P_2P_2', respectively. These findings may improve the efficiency and efficacy of extra-muscular neurolysis and intramuscular chemodenervation using botulinum toxin A to treat brachioradialis muscle spasticity.

Keywords: Brachioradialis muscle, spasticity, nerve entry point, intramuscular nerve-dense regions, blocking targets localization

Introduction

Patients with conditions such as stroke, brain trauma, spinal cord injury, multiple sclerosis, cerebral palsy, and other disabling neurological diseases often present with various degrees of spasticity as the disease progresses. Patients frequently exhibit increased muscle tension of the upper limb flexor and lower limb extensor muscles, namely the Wernicke-Mann posture, which is a physiological consequence of injury to the brain or spinal cord that can cause life-threatening disability and incur high costs [1, 2]. Currently, many techniques and drugs are available for the treatment of spasticity, such as extra-muscular neurolysis and intramuscular chemodenervation [3, 4]. The former refers to the injection of alcohol or phenol into the neural trunk or nerve entry point (NEP), which causes degeneration of the nerve sheaths or axons, thereby reducing local muscle-nerve activity [5]. The latter involves the injection of botulinum toxin A (BTX-A) into the intramuscular motor points (motor endplate zones), which blocks the presynaptic release of acetylcholine and thus inhibits muscle excitation [6]. Although these two methods employ palpation, electromyography, ultrasound, and electrical stimulation, which can induce some therapeutic effects [7-9], they have limitations of differing degrees. Clinicians still cannot accurately localize the puncture target and determine the depth of the muscle target to avoid exploratory puncturing for confirmation, thus exacerbating patients' pain, which may result in unnecessary complications. To this end, accurate localization of the NEP and intramuscular motor points are considered critical for the successful implementation of these two treatment methods.

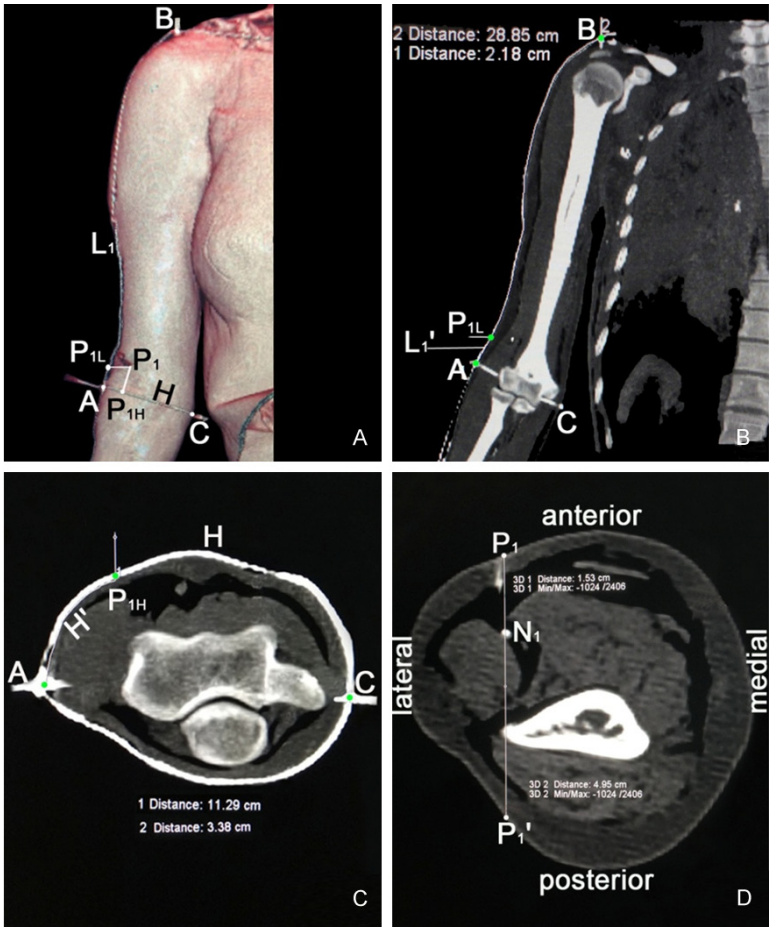

Figure 1. The corresponding surface location and depth of the nerve entry point (NEP) of the brachioradialis muscle were determined by spiral computed tomography (CT). A. A three-dimensional reconstructed spiral CT image showing the relationship between the location of the NEP and bony landmarks. B. The curve lengths of L_1 and L_1' were measured on coronal images. C. The lengths of the curved lines H and H' were measured on cross-sectional images. D. The percentage puncture depth on a cross-sectional CT image of the NEP of the brachioradialis muscle.

In addition to the biceps brachii and brachialis muscles, the brachioradialis muscle is critical to the development of spasticity of the elbow flexor [10]. The location of the NEPs of the biceps brachii and brachialis muscles has been described in a gross anatomy study [11]; the locations of the intramuscular nerve-dense regions (INDR) of these two muscles were the same as that of the motor endplate zone [12]. Although the brachioradialis has a fine-tuning role in relation to the biceps brachii muscle [13], studies investigating the brachioradialis have been ignored by researchers in the fields of NEP and INDR. To improve elbow joint movement by relieving brachioradialis muscle spasticity, as well as to maximize the effectiveness and minimize puncture pain and side effects, the location of the NEP and INDR of the brachioradialis muscles must be accurately localized.

Therefore, the purpose of this study was to use gross anatomy to expose the NEP and then use the modified Sihler's staining method to identify the INDR of the brachioradialis muscle and barium sulfate to mark them to utilize spiral computed tomography (CT) scanning and three-dimensional (3D) reconstruction to accurately localize the body surface location and puncture depth of the NEP and center of the INDR (CINDR) in the brachioradialis muscle. Our findings provide anatomical guidance to improve the efficiency and efficacy of the treatment of elbow flexor spasticity.

Materials and methods

Specimens and ethics

This study was conducted using the upper limbs of 20 formalin-fixed adult cadavers of individuals (15 men, 5 women) who were aged 35-80 years at the time of death. None of the subjects had a history of neuromuscular disease or upper-limb joint deformation. This experiment was approved by the ethical committee of our college.

Gross anatomy and reference line design

According to our observations of the location of the brachioradialis muscular branch in anatomical teaching, the lateral epicondyle of the humerus (A), the acromion (B), the medial epicondyle of the humerus (C), and the styloid process of the radius (D) were chosen as bony landmarks for designing a reference line (**Figure 1A-C**). Each cadaver was placed in the supine position. One longitudinal incision was made

along the line from the acromion to the radial styloid process after crossing the lateral epicondyle of the humerus. Two transverse incisions were subsequently made along the lines that joined the acromion to the jugular notch and the radial styloid process to the ulnar styloid process, respectively. The skin and superficial fascia were treated as one layer, and the surface of the muscle was exposed. A measuring tape was used to measure the muscle length from the nearest origin to the farthest insertion of the muscle fibers. At the top of the elbow joint, the brachioradialis muscular branch was exposed between the brachioradialis and brachialis muscles. The number of nerve branches, their passage and location of muscle entry, and the presence of blood vessels were observed and noted.

To facilitate the description of the NEP and CINDR of the brachioradialis muscle, these two points were named N_1 and N_2, respectively. To describe the superoinferior and mediolateral relationship between N_1 and N_2 and the bony landmarks, the curved lines joining the lateral epicondyle of the humerus and acromion and the lateral epicondyle of the humerus and radial styloid process were designated as the longitudinal reference lines, L_1 and L_2, of the N_1 and N_2, respectively. In the anterior plane of the elbow, the curved line joining the lateral and medial epicondyles of the humerus was designated as the common horizontal reference line (H) for N_1 and N_2 (**Figures 1A-C** and **4A-C**).

NEP localization

After the brachioradialis nerve branches in the 10 right and 10 left upper limbs were exposed, barium sulfate combined with 801 glue (Wenzhou 801 Glue Co. Ltd., Wenzhou, China) (1 mL glue to 4 g medical barium sulfate powder) was used to stain the distal nerve branch over a 0.5-cm area. The barium sulfate mixture was dried using heat, and incisions were closed in layers. A needle was inserted at each of the three A, B, and C landmarks, and then the AB and AC landmarks on the skin were sutured using barium sulfate-soaked silk thread to represent the L_1 and H lines, respectively (**Figure 1A-C**). Spiral CT scanning was conducted using a 64-row scanner (Siemens, Munich, Germany) (collimation = 64 × 1, slice thickness = 1 mm, pitch = 1:1, current = 120 kV with automatic mA adjustment, thin layers with 3D image reconstruction), and 3D reconstruction was performed in cross-sections using a Syngo system (Siemens). Using the cross-sectional images, the first white point that appeared from the upper limb, from the distal to proximal end, (i.e., the end of the nerve muscle branch labeled with barium sulfate) was considered to represent the NEP (**Figure 1D**). Using the same indicator, with the aid of CT scanning and a needle punctured through the skin perpendicular to the coronal plane, the projection point (P_1) of the NEP (N_1) was located on the body surface, which was the puncture point. Following repeated CT scanning, 3D reconstruction, and the use of curve measurement tools, the lengths of L_1 and H were measured along the coronal and cross-skin surfaces, respectively (**Figure 1B** and **1C**). The intersection point of the horizontal line and line L_1 through P_1 was designated as P_{1L}; the intersection point of the straight line parallel to the axis of the arm and line H through P_1 was designated as P_{1H}; the length of the curved line between A and P_{1L} was designated as L_1'; and the length of the curved line between A and P_{1H} was designated as H' (**Figure 1A-C**). The ratios of H'/H and L_1'/L_1 were calculated and expressed as percentages; P_{1L} and P_{1H} of P_1 on the body surface were determined in percentage values. In the cross-sectional images, the P_1 by N_1 projecting to the skin of the opposite direction was designated as P_1'. P_1N_1 and P_1P_1' were measured using a linear tool (**Figure 1D**), and $P_1N_1/P_1P_1' \times 100\%$ was calculated to determine the puncture depth.

INDR staining and CINDR localization

Following NEP localization, the 20 samples of the brachioradialis muscles were harvested. Intramuscular nerve staining was performed in accordance with the modified Sihler's method, as previously described [14, 15]. Briefly, brachioradialis muscles were macerated for 4-5 weeks in 3% potassium hydroxide and 0.2% hydrogen peroxide solution, decalcified for 4 weeks in Sihler's I solution, stained for 4 weeks in Sihler's II solution, decolored for 3-10 h in Sihler's I solution, neutralized for 2 h in 0.05% lithium carbonate solution, and subjected to a glycerol gradient for 1 week (40%, 60%, 80%, and 100%) to achieve transparency. The branches and distribution of the intramuscular nerves were carefully observed and photographed, and a pattern was drawn under the radiographic film lamp. Subsequently, the area

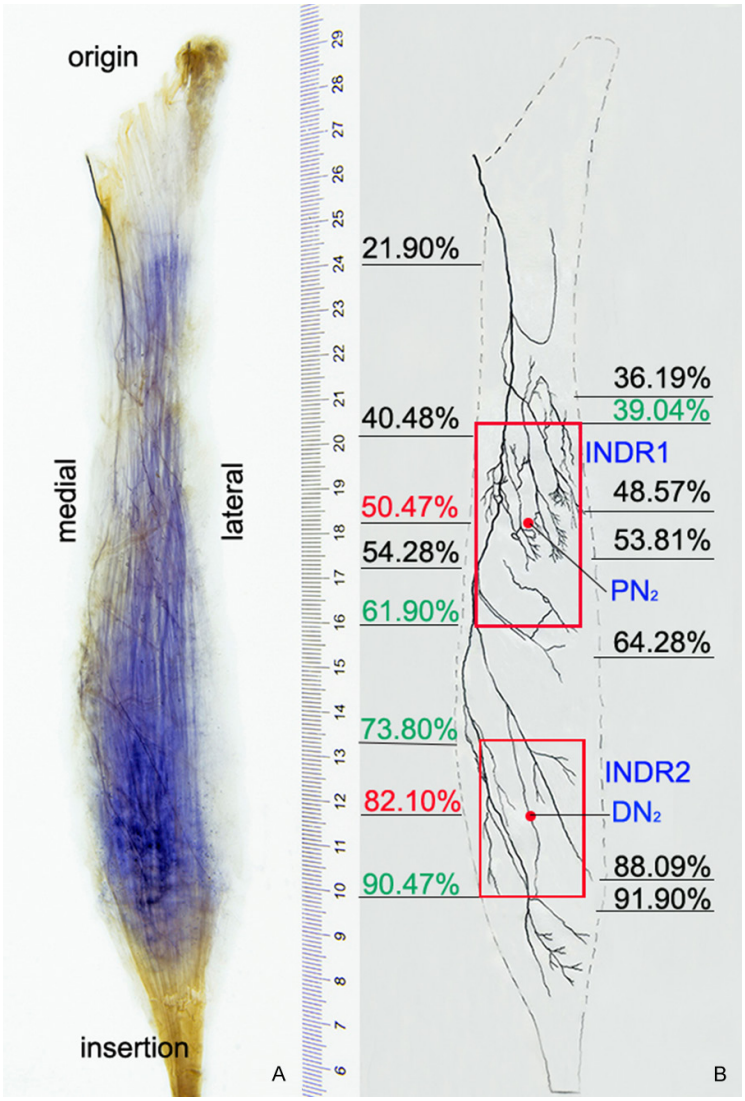

Figure 2. Sihler's staining showing the distribution pattern and location of the intramuscular nerves in the brachioradialis muscle (superficial view). (A) Representative image of intramuscular nerve staining. (B) Schematic drawing of (A) showing the distribution of the intramuscular nerves. The two red boxes represent the proximal and distal intramuscular nerve-dense regions (INDR), respectively. PN_2 and DN_2 represent the centers of these two regions, respectively.

of the INDR was measured using a vernier caliper, and the percentage location of CINDR (N_2) was calculated according to the muscle length, width, and thickness. The contralateral brachioradialis muscles were exposed (10 left and 10 right), and the muscle length, thickness, and width were measured at the corresponding percentile of N_2. A syringe was used to inject barium sulfate-containing glue into the center of the muscle belly prior to CT scanning, and the following parameters were named and determined according to the NEP localization method: proximal P_2 (PP_2), distal P_2 (DP_2), PP_{2L}, DP_{2L}, PP_{2H}, DP_{2H}, $H'/H \times 100\%$, $L_2'/L_2 \times 100\%$, and $P_2N_2/P_2P_2' \times 100\%$. The percentage distance of the N_2 projection on the body surface and its puncture depth were determined (**Figure 4A-D**). The 20 brachioradialis muscle samples were then subjected to Sihler's staining to verify whether the distribution pattern of the intramuscular nerves and the location of the CINDR were consistent with those of the contralateral side.

Statistical analysis

Target locations were expressed as percentages ($\bar{x} \pm S$) % to eliminate the effect of individual differences in height and weight. Data from the left and right sides were compared using the paired t-test. The significance level was $\alpha = 0.05$.

Results

Anatomical observation and measurement

After the radial nerve exits the humeromuscular tunnel above the lateral epicondyle of the humerus between the brachialis and brachioradialis muscles, it inferolaterally projects 1-2 brachioradialis muscle branches (93.33% of 1-branch type) at 18.09% of the muscle length (25.10 ± 2.24 cm) medial to the profundal surface into the muscle. There were no blood vessels in the NEP. The thickness of the brachioradialis muscle was 0.27 ± 0.03 cm.

Location of the NEP

The NEP and reference line were marked by barium sulfate, and the bony landmarks appeared white on images. The needle puncture point indicated the body surface position of the NEP. P_{1L} and P_{1H} of P_1 were located at 9.33 ± 0.55% and 30.69 ± 1.96% of the L_1 and H

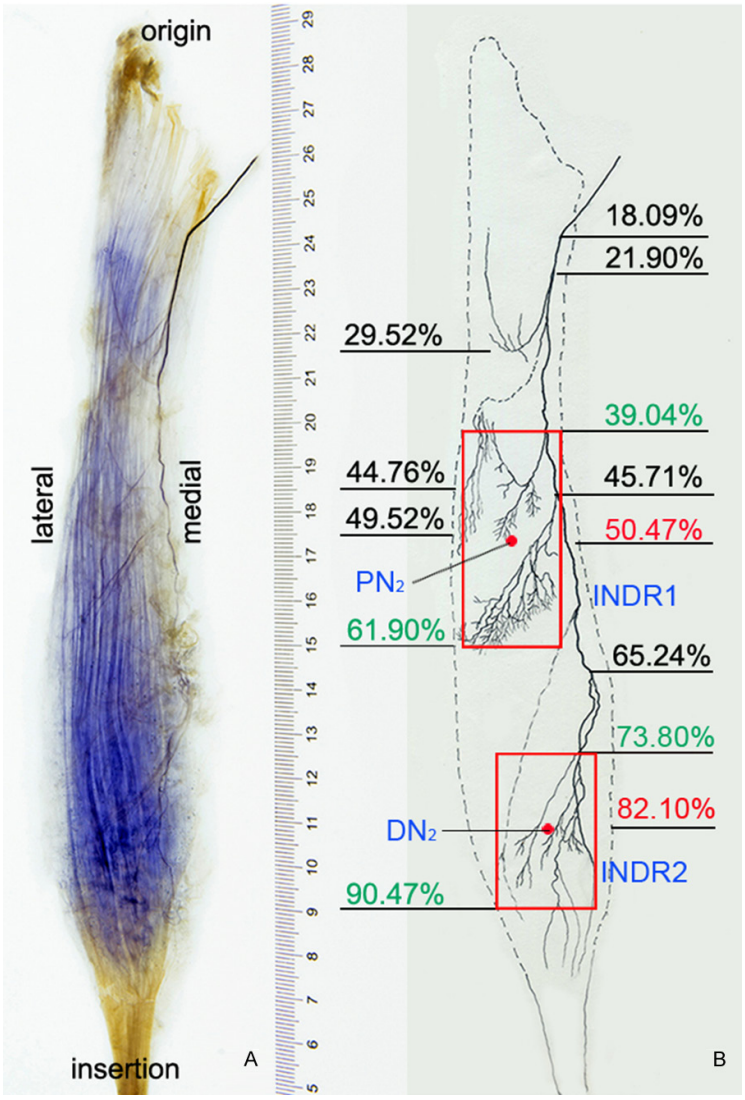

Figure 3. Sihler's staining showing the distribution pattern and location of the intramuscular nerves of the brachioradialis muscle (profundal view). (A) Representative image of intramuscular nerve staining. (B) Schematic drawing of (A) showing the profundal distribution locations of the proximal and distal intramuscular nerve-dense regions (INDRs) in the brachioradialis muscle.

lines, respectively. The puncture depth was located at 31.03 ± 1.19% of the P_1P_1' line (**Figure 1A-D**). A total of 10 right and left sides were compared and demonstrated no statistically significant difference (P = 0.16).

Distribution patterns of the intramuscular nerves

The brachioradialis muscle nerve branches were stained with black and projected to the distal end along the medial edge of the muscle, which extended four primary nerve branches in the superficial and deep surface layers of the muscle from the superomedial to inferolateral direction, respectively.

At the superficial surface of the muscle, the first primary branches formed at 21.90% of the muscle length (upper part), which divided into two secondary branches at 36.19%. The lateral secondary branch projected abundant arborized branches along the way and distributed to 48.57% of the lateral region of the muscle. The medial secondary branches also projected arborized branches and distributed to 53.81% of the lateral region of the muscle. The second primary branch was observed at 40.48% of the muscle length (middle part); anastomosis was detected between its dense arborized branches and the medial secondary branch of the first primary branch, and its terminal branches distributed to 53.81% of the center of the muscle. The third primary branches were noted at 54.28% (middle part) of the muscle length; its branches were anastomosed with the deep branches, and the terminal branches distributed to 64.28% of the lateral length of the muscle. The fourth primary branches were detected at the 61.90% level of the muscle (middle portion) and obliquely projected to 88.09% of the lateral length of the muscle, which mainly innervated the lower part of the lateral muscle fibers. When the primary branch targeted the muscle belly at the center, one secondary branch ran parallel to the long axis of the muscle and innervated at the distal part of the muscle, forming a U-type communication with the terminal branches of the nerve trunk. The terminal branches of the nerve trunk innervated half of the medial part of the lower muscle and became a tendon branch at 91.90% of the length (**Figure 2A**, **2B**).

At the deep surface of the muscle, the first primary branch projected at 21.90% of the muscle length (upper part) and obliquely traveled to

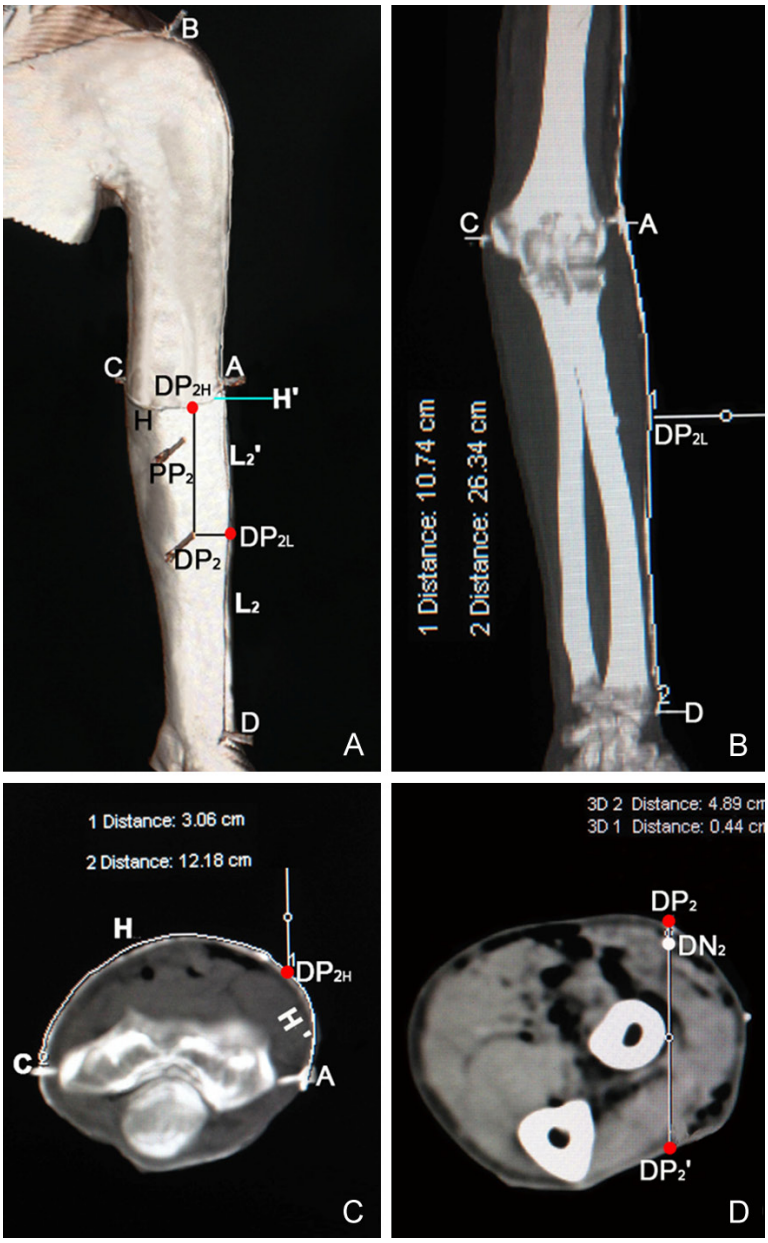

Figure 4. Corresponding surface locations and depths of the centers of the intramuscular nerve-dense regions (CINDRs) were determined by spiral computed tomography (CT). A. A three-dimensional reconstructed spiral CT image showing the relationship between the body surface projection location (PP_2 and DP_2) of the CINDRs and the bony landmarks. DP_{2L} and DP_{2H} represent the intersections of the distal P_2 and L_2 with the H line, respectively. B. The lengths of the curved lines L_2 and L_2' were measured on coronal images (DN_2 is shown as an example). C. The lengths of the curved lines H and H' were measured for DN_2 on cross-sectional images. D. The percentage puncture depth of DN_2 on a cross-sectional CT image.

the 29.52% level of the muscle belly and turned lateral to superior in a U-shape back to the proximal side of the muscle. The second primary branch projected off at 39.04% of the muscle length (middle part) and then branched into a secondary branch at 44.76% of the center of the muscle that traversed to 49.52% from the center of the muscle. The third primary branch was observed at 45.71% of the muscle length (middle part), reaching the lateral margin at 61.90% of the muscle length. The arborized branches of this primary branch were the densest. The fourth primary branch branched off at 65.24% of the muscle length (middle part), toward the inferolateral direction, projected arborized branches along the way, and became a tendon branch at the 90.47% level of the center of the muscle (**Figure 3A**, **3B**).

Depending on whether the muscle depth was superficial or deep, the nerve branches of the two regions at 39.04-61.90% and 73.80-90.47% of the muscle length were typically the densest; the areas of these two dense regions were 10.08 ± 0.25 cm^2 and 8.05 ± 0.32 cm^2, respectively. The proximal N_2 (PN_2) was located at 50.47 ± 0.45% of the muscle length, and the distal N_2 (DN_2) was located at 82.10 ± 0.96% of the muscle length. The intramuscular nerve distribution pattern, demonstrated by Sihler's staining, of one side differed slightly (5%) from the contralateral side in the 20 brachioradialis muscle samples labeled by barium sulfate glue. The location of the CINDR did not significantly differ between sides (P = 0.11).

CT localization of the CINDR

The percentage location of the intersections (PP_{2L} and DP_{2L}) of the PP_2 and DP_2 and L_2 line were located at 12.60 ± 0.49% and 40.74 ± 1.07% of L_2 respectively, and the percentage location of the intersections (PP_{2H} and DP_{2H}) of

the PP_2 and DP_2 and H line were located at 25.12 ± 0.63% and 32.86 ± 0.77% of H, respectively. The puncture depth of the PN_2 and DN_2 were located at 5.99 ± 0.40% of the proximal P_2P_2' and 8.99 ± 0.38% of the distal P_2P_2', respectively. **Figure 4A-D** shows the CT localization of DN_2. Comparison of the data from the left and right sides revealed no statistically significant difference between sides (P = 0.09).

Discussion

Spasticity is a common clinical manifestation of injuries to the central nervous system. In patients with upper-limb muscular spasticity, elbow flexion deformity may lead to difficulty reaching, dressing, and retrieving items [4]. Currently, a popular approach is to break the pattern of this spasticity and promote the activity of the limb as soon as possible via specialized movements to relieve pain and restore patients' activities of daily living.

Percutaneous phenol blockade of the musculocutaneous nerve has been reported to control spasticity of the biceps brachii and brachialis muscles and improve elbow extension function [16]. Involvement of the brachioradialis muscle has been demonstrated in elbow flexion spasticity; however, the exact location of the brachioradialis muscle NEP has not yet been defined. Therefore, the accurate anatomical localization of the brachioradialis muscle NEP is particularly important for the successful injection of phenol or alcohol for the neurolysis of brachioradialis muscle spasticity. This knowledge could also help to avoid repeated injections, which may lead to muscle fibrosis and contracture, paresthesia, non-spastic muscle involvement, and other side effects. The results of this study suggest that if a physician intends to use neurolysis for the treatment of brachioradialis muscle spasticity, the length of the curved line from the lateral epicondyle of the humerus to the acromion should first be measured using measuring tape held close to the skin. Then, one horizontal line should be made at 9.33 ± 0.55% of this line. Following this, the length of the curved line from the lateral epicondyle to the medial epicondyle of the humerus should be measured, and one parallel line should be drawn to the arm axle at 30.69 ± 1.96% of this line. The intersection of these two lines on the skin is the puncture point (P_1). Finally, the length of P_1P_1' should be measured using a pelvis-measuring instrument once P_1 is perpendicular to thecoronal plane. The depth of puncture can be obtained by multiplying by 31.03 ± 1.19%. These parameters will improve the efficiency and efficacy of neurolysis for brachioradialis muscle spasticity.

Previous studies have shown that the accurate injection of 51.6 ± 26.8 units of BTX-A into the brachioradialis muscle could not only relieve muscle spasticity and movement limitation, but may also improve upper-limb function [10, 17]. Locating the target muscle by simple palpation and surface anatomy is a simple and acceptable method for large and superficial muscles. Although the brachioradialis muscle is a narrow, superficial muscle, the accuracy of this technique in the forearm muscles is quite low, ranging from 13% to 35% [18]. To improve accuracy, the activation of small intramuscular nerve branches using electrical stimulation is required to place the needle as close as possible to the neuromuscular junctions, as even a minor stimulus can induce a large twitch [19, 20]. Therefore, to reduce the trial-and-error of multiple punctures, which causes pain to patients, and determine the most effective and safe injection point for BTX-A into the brachioradialis muscle, the brachioradialis muscle requires more specific anatomical investigation.

Motor endplates are typically located in the center of the muscle fibers. The middle portion of a long muscle, which is formed by isometric muscle fibers, is the thickest part, and the motor endplate is visible [21]. Therefore, BTX-A is generally injected into the middle of the muscle belly or the thickest portion of the muscle. However, as is apparent from our results, extra- and intramuscular innervation of the brachioradialis muscle was not observed in this area. Depending on the brachioradialis muscle depth, the brachioradialis muscle was shown to have four primary nerve branches that form dense nerve-distribution regions. In particular, the two regions at 39.04-61.90% and 73.80-90.47% of the muscle length demonstrated the densest innervation, suggesting that this muscle did not possess a single dense innervation band. These findings are consistent with the brachioradialis muscle having a series-fibered architecture consisting of multiple, overlapping bands of muscle fibers in most individuals [22].

As injection of BTX-A blocks spasticity via dose-dependent chemical denervation; once BTX-A is injected into the muscle, it will immediately spread in the vicinity of the needle tip within a few centimeters [23]. Therefore, in this study, the center (50.47 and 82.10%) of each area 39.04-61.90% and 73.80-90.47% of the muscle length was considered the target point for localization. These results suggested that physicians who intend to inject BTX-A for the treatment of brachioradialis muscle spasticity should first measure the length of the curved line from the lateral epicondyle of the humerus to the styloid process of the radius using a measuring tape held close to the skin. One horizontal line should then be made at 12.60 ± 0.49% and 40.74 ± 1.07% of this line, respectively. Subsequently, the curved line should be measured from the lateral epicondyle to the medial epicondyle of the humerus, and one vertical line should be made at 25.12 ± 0.63% and 32.86 ± 0.77% of this line, respectively. The intersection of these two lines on the skin indicates the surface projection of the proximal and distal CINDR, respectively; i.e., the puncture points (PP_2 and DP_2). Finally, the length of P_2P_2' should be measured using a pelvis-measuring instrument after P_2 is established perpendicular to the coronal plane. The depth of the PN_2 and DN_2 can be obtained by multiplying P_2P_2' by 5.99 ± 0.40% and 8.99 ± 0.38%, according to the neuromuscular junctions in the brachioradialis muscle. These parameters will improve the efficiency and efficacy of BTX-A chemo-denervation for elbow flexion spasticity. Previous studies have shown that one unit of BTX-A can infiltrate 1.5-3 cm, and 2.5-5 units of BTX-A can infiltrate 4.5 cm [24]. Our results demonstrated that the areas of the brachioradialis muscle INDRs were 10.08 ± 0.25 and 8.05 ± 0.32 cm^2, respectively, indicating that with accurate injection, only 4-7 units of BTX-A will have a good effect, and there is no need to inject 51.6 ± 26.8 units.

In conclusion, this study used barium sulfate staining, along with spiral CT 3D reconstruction and reference lines designed with bony landmarks, to identify the NEP and CINDR of the brachioradialis muscle. The NEP and CINDR were located on the body surface, and the puncture depth was determined geometrically. Data were collected by measuring the curved lines close to the skin and expressed as relative percentages. The results obtained are accurate and clinically relevant and provide scientific guidance for improving the efficiency and efficacy of the treatment of elbow flexor spasticity. For clinical applications, this study also provides guidance for reducing the number of exploratory punctures, if the target is localized with an electrical stimulator or electromyogram. However, a limitation of this study is that our observations were limited to cadaver samples. These findings require further confirmation via clinical investigations.

Acknowledgements

The authors would like to acknowledge Shuangjiang Hu and Xufeng Tian for their excellent technical assistance and use of their spiral CT laboratory. This work was supported by the National Natural Science Foundation of China (31540031) and the Provincial Natural Science Joint Foundation of Guizhou (LH-2015-7528).

Disclosure of conflict of interest

None.

Address correspondence to: Shengbo Yang, Department of Anatomy, Zunyi Medical College, 201 Dalian Road, Zunyi 563000, Guizhou Province, People's Republic of China. Tel: +8615885627077; Fax: +868528609666; E-mail: yangshengbo8205486@163.com

References

[1] Ward AB. Spasticity treatment with botulinum toxins. J Neural Transm (Vienna) 2008; 115: 607-616.

[2] Hefter H, Jost WH, Reissig A, Zakine B, Bakheit AM, Wissel J. Classification of posture in poststroke upper limb spasticity: a potential decision tool for botulinum toxin A treatment? Int J Rehabil Res 2012; 35: 227-233.

[3] Francisco GE, McGuire JR. Poststroke spasticity management. Stroke 2012; 43: 3132-3136.

[4] Slovak M, Chindo J, Nair KP, Reeves ML, Heller B, Barker AT. Sensory barrage stimulation in the treatment of elbow spasticity: a crossover double blind randomized pilot trial. Neuromodulation 2016; 19: 220-226.

[5] Kocabas H, Salli A, Demir AH, Ozerbil OM. Comparison of phenol and alcohol neurolysis of tibial nerve motor branches to the gastrocnemius muscle for treatment of spastic foot after stroke: a randomized controlled pilot study. Eur J Phys Rehabil Med 2010; 46: 5-10.

[6] Isner-Horobeti ME, Muff G, Lonsdorfer-Wolf E, Deffinis C, Masat J, Favret F, Dufour SP, Lecocq J. Use of botulinum toxin type A in symptomatic accessory soleus muscle: first five cases. Scand J Med Sci Sports 2016; 26: 1373-1378.
[7] Boudarham J, Hameau S, Pradon D, Bensmail D, Roche N, Zory R. Changes in electromyographic activity after botulinum toxin injection of the rectus femoris in patients with hemiparesis walking with a stiff-knee gait. J Electromyogr Kinesiol 2013; 23: 1036-1043.
[8] Kawashima N, Popovic MR, Zivanovic V. Effect of intensive functional electrical stimulation therapy on upper-limb motor recovery after stroke: case study of a patient with chronic stroke. Physiother Can 2013; 65: 20-28.
[9] McGuire J, Heath K, O'Dell MW. Should ultrasound be used routinely to guide botulinum toxin injections for spasticity? PM R 2016; 8: 1004-1010.
[10] Horimoto Y, Inagaki A, Yoshikawa M, Kanbe K, Tanaka H, Ando R, Hibino H, Tajima T, Fukagawa K, Kabasawa H. Therapeutic outcome of onabotulinum toxin type A in patients with upper limb spasticity. Rinsho Shinkeigaku 2015; 55: 544-549.
[11] Park BK, Shin YB, Ko HY, Park JH, Baek SY. Anatomic motor point localization of the biceps brachii and brachialis muscles. J Korean Med Sci 2007; 22: 459-462.
[12] Lee JH, Kim HW, Im S, An X, Lee MS, Lee UY, Han SH. Localization of motor entry points and terminal intramuscular nerve endings of the musculocutaneous nerve to biceps and brachialis muscles. Surg Radiol Anat 2010; 32: 213-220.
[13] Von Werder SC, Disselhorst-Klug C. The role of biceps brachii and brachioradialis for the control of elbow flexion and extension movements. J Electromyogr Kinesiol 2016; 28: 67-75.
[14] Xie P, Jiang Y, Zhang X, Yang S. The study of intramuscular nerve distribution patterns and relative spindle abundance of the thenar and hypothenar muscles in human hand. PLoS One 2012; 7: e51538.
[15] Xie P, Xue Q, Zhang Y, Zhang X, Yang S. The study of intramuscular nerve distribution pattern of various skeletal muscles in rabbit. Journal of Neurological Sciences 2013; 30: 525-531.
[16] Keenan MA, Tomas ES, Stone L, Gerstén LM. Percutaneous phenol block of the musculocutaneous nerve to control elbow flexor spasticity. J Hand Surg Am 1990; 15: 340-346.
[17] Turner-Stokes L, Fheodoroff K, Jacinto J, Maisonobe P. Results from the upper limb international spasticity study-II (ULISII): a large, international, prospective cohort study investigating practice and goal attainment following treatment with botulinum toxin A in real-life clinical management. BMJ Open 2013; 3: e002771.
[18] Chin TY, Nattrass GR, Selber P, Graham HK. Accuracy ofintramuscular injection of botulinum toxin A injuvenile cerebral palsy: a comparison between manual needle placement and placement guided by electrical stimulation. J Pediatr Orthop 2005; 25: 286-291.
[19] Park ES, Rha DW. Botulinum toxin type A injection for management of upper limb spasticity in children with cerebral palsy: a literature review. Yonsei Med J 2006; 47: 589-603.
[20] Won SY, Hur MS, Rha DW, Park HD, Hu KS, Fontaine C, Kim HJ. Extra- and intramuscu-lar nerve distribution patterns of the muscles of the ventral compartment of the forearm. Am J Phys Med Rehabil 2010; 89: 644-652.
[21] Happak W, Liu J, Burggasser G, Flowers A, Gruber H, Freilinger G. Human facial muscles: dimensions, motor endplate distribution, and presence of muscle fibers with multiple motor endplates. Anat Rec 1997; 249: 276-284.
[22] Lateva ZC, McGill KC, Johanson ME. The innervation and organization of motor units in a series-fibered human muscle: the brachioradialis. J Appl Physiol 2010; 108: 1530-1541.
[23] Kinnett D. Botulinum toxin A injections in children: technique and dosing issues. Am J Phys Med Rehabil 2004; 83: S59-64.
[24] Borodic GE, Ferrante R, Pearce LB, Smith K. Histologic assessment of dose-related diffusion and muscle fiber response after therapeutic botulinum A toxin injections. Mov Disord 1994; 9: 31-39.